

## Modified Biopolymer as Adsorbent for Methylene Blue Dye Removal

A. Belaid<sup>a</sup>, T. Hocine<sup>a</sup>, B. Bouras<sup>a,\*</sup>, L. Tennouga<sup>a</sup>, K.I. Benabadji<sup>a</sup> and K. Benhabib<sup>b</sup>

<sup>a</sup>Laboratory of Organic Electrolytes and Polyelectrolytes Application (LAEPO), Department of Chemistry, Faculty of Science, Tlemcen University, B. P. 119 13000 Tlemcen, Algeria

<sup>b</sup>Eco-Processes, Optimization and Decision Support (EPROAD, EA), University of Picardie Jules Verne, IUT of Aisne, 48 rue d'Ostende, 02100 Saint-Quentin, France

(Received 16 April 2023, Accepted 17 June 2023)

In this work, we developed an eco-friendly material for use in the wastewater treatment operation. A copolymer was prepared from carboxymethylcellulose (CMC) modified with acrylamide (AM) and N-vinylpyrrolidone (NVP). Then, it was characterized using FTIR spectrometry, thermogravimetric analysis (TGA/DTG) and diffraction of X-ray (XRD). The properties of CMC-AM-NVP copolymer as an adsorbent of methylene blue (MB) dye were investigated and the parameters affecting the removal process were evaluated. It was found that the adsorption of MB dye on the CMC-AM-NVP copolymer can be described by the pseudo-second order equation. Equilibrium data was modeled by Langmuir, Freundlich, and Temkin isotherms. Langmuir isotherm model provided the best fit for the adsorption of MB on the CMC-AM-NVP copolymer with  $R^2$  value of 0.999. The efficiency of dye elimination on the copolymer reached 99.4%. The study outcomes show that CMC-AM-NVP is a promising candidate for efficient removal of methylene blue; therefore, it is concluded that the addition of NVP to the copolymer has a notable improvement in the adsorption process.

**Keywords:** Carboxymethylcellulose (CMC), Acrylamide (AM), N-vinylpyrrolidone (NVP), Adsorption

### INTRODUCTION

Securing the availability of clean water to the global population is one of the significant challenges of the future. The rise in the population and water contamination has a direct effect on the quality of water. Today's industrial dyes are becoming a troublesome class of environmental contaminants. Owing to their complex nature, the discharge of dyes in water resources has poor aesthetic and health consequences [1]. Due to the large amounts of water needed in dyeing operations, the textile sector is one of the biggest producers of liquid effluent pollutants [2]. In addition, the different effluent characteristics in terms of pH, dissolved oxygen, and organic and inorganic chemical content depend on the processing steps and species of synthetic dyes used

during this industrial conversion.

The processes or technologies available to remove the dyes tuffs from the textile liquid effluent are diverse. These processes require the mediation of a few physical-compound strategies, for example, coagulation-flocculation, synthetic oxidation [3], film division [4], organic treatment [5], etc. The failure of the regular cycles to productive disposal of numerous unmanageable, harmful mechanical items, or their significant expense verifies that it is essential to consider high-effective methods with minimal conceivable expenses. Adsorption is a valuable method for removing toxic dyes from wastewater. Consequently, there has been an increased interest in adsorbents that are renewable, affordable, accessible, and highly effective [6]. Various investigations have indicated the utilization of various adsorbents to decrease the color fixations from aqueous arrangements. Materials such as activated carbon [7], modified bentonite [8], quaternized poly(4-vinylpyridine) copolymers [9],

\*Corresponding author. E-mail: [bourasbrahim\\_m8@yahoo.fr](mailto:bourasbrahim_m8@yahoo.fr)

composites [10], and polysaccharide-based hydrogels [11] have shown many exciting applications.

Numerous copolymers based on polysaccharides, such as carb CMC, have been created recently. Their functional properties including high hydrophobicity, biodegradability, and biocompatibility have made them suitable for use in water treatment in diverse industrial effluents [12]. Many researchers have made great efforts to model CMC with vinylic or acrylic monomers to improve the adsorption performance of organic particles on CMC-based materials. Feng *et al.* modified CMC with AM monomer for use in the coagulation-flocculation process, and they found that grafting of PAM in CMC hydrogel can significantly improve the coagulation process [13]. Godiya *et al.* developed the CMC/PAM hydrogel for ion adsorption ( $\text{Cu}^{\text{II}}$ ,  $\text{Pb}^{\text{II}}$ , and  $\text{Cd}^{\text{II}}$ ) and found a better ion adsorption capacity compared to the conventional adsorbents such as activated carbon and cation exchange resin [14]. In order to enhance the efficiency of flocculation in the treatment of coal mine effluent, Zou *et al.* developed a cationic material by grafting the acrylamide onto the pea starch, and they found that the prepared material may be applied as a novel flocculant [15].

This paper outlines a new approach to modify the carboxymethyl cellulose (CMC) with Acrylamide (AM) and N-vinylpyrrolidone (NVP) monomers. The obtained copolymer was employed as an adsorbent for removing cationic dye (Methylene Blue). The effects of several experimental parameters were studied to optimize the adsorption conditions. To assess the adsorption process, some kinetic studies were carried out.

## EXPERIMENTAL

### Materials

Carboxymethylcellulose (CMC) used was supplied by

PROLABO (France). Its degree of carboxymethylation values was included between [0.82-0.95], given by PROLAB, and its average molecular weight was determined by viscometry technique as  $M_v \approx 316400 \text{ g mol}^{-1}$  [16]. N-vinyl pyrrolidone (NVP, 98%) was provided by Aldrich (USA), and acrylamide (AM) compound was purchased from Merck (France) and used as received. Methylene Blue (MB) was purchased from Sigma-Aldrich (USA) and used without further purification. The properties of MB are shown in Table 1.

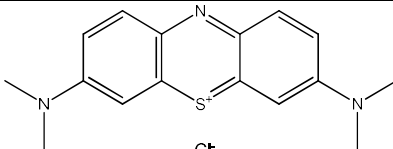
### CMC-AM and CMC-AM-NVP Copolymers Preparation

A quantity of CMC was dissolved in a volume of bidistilled water. This solution was stirred for 30 min at 80 °C. An aqueous ammonium persulfate solution [APS] was separately prepared according to the desired concentration in a tube at room temperature, and it was added as an initiator. In 25 ml of bidistilled water, acrylamide and N-vinylpyrrolidone monomers were dissolved. After homogenizing the reagent solution, the mixture was allowed to reflux. The obtained product was precipitated in ethanol, filtered and dried.

### Batch Adsorption Studies: Removal of MB Dye from the Aqueous Solution

The MB adsorption capacities of the prepared copolymers were evaluated using a batch equilibrium procedure. First, MB solutions ( $1 \text{ g l}^{-1}$ ) were prepared in distilled water as a mother solution. The desired concentration series were obtained by dilution. Next, 25 mg of copolymers was added to each of the 40 ml dye solutions. The adsorption experiments were carried out in beakers at a constant stirring rate of 400 rpm, the solution's pH range from 2 to 11 (the desired pH has been set by adding drops of NaOH

**Table 1.** Physicochemical Characteristics of Methylene Blue (MB)

Name	Molecular structure	Nature	$M_w$ ( $\text{g mol}^{-1}$ )	$\lambda_{\text{max}}$ (nm)
Methylene Blue (Basic Blue 9)		Cationic	319.851	664

or HCl solution (1 M)), the temperature between 25 and 55 °C, the contact time between 2 and 180 min, the amount of adsorbent between 5 and 45 mg, and the initial dye concentration from 5 to 300 mg l<sup>-1</sup>. The solutions were left to settle for 5 min, and the supernatant was dosed by OPTIZEN 1412 UV/VIS spectrophotometer at  $\lambda = 664$  nm, for MB. Finally, adsorption capacities ( $q_e$ ) of these copolymers were determined by the Eq. (1): [8]

$$q_e = \frac{(C_0 - C_e) V}{m} \quad (1)$$

### Characterization

Thermogravimetric analysis of the copolymers was obtained by TGA (TA Instruments Q Series Q600 SDT). Infrared spectra were performed with an Agilent Cary 600 series FTIR spectrometer. In addition, The XRD patterns of the copolymers were made with the ULTIMA IV X-ray diffractometer, working with K $\alpha$  copper radiation ( $\lambda = 1.54$  Å) at 40 kV and 30 mA. Scanning electron microscopy SEM was made with the HITACHI TM-1000 electron microscope. All the methods of characterization were performed according to the same experimental condition described in our earlier work [17].

### Determination of $pH_{pzc}$

The zero-charge point ( $pH_{pzc}$ ) is an important factor to investigate adsorption efficiency. It was carried out according to the method described in the previous work [8].

## RESULTS AND DISCUSSION

### Characterization

**Infrared spectroscopy (FTIR).** The FTIR of carboxymethylcellulose (CMC), carboxymethylcellulose-acrylamide (CMC-AM), and carboxymethylcellulose-acrylamide-N-vinylpyrrolidone (CMC-AM-NVP) copolymers are presented in Fig. 1

The peaks at 3435 cm<sup>-1</sup> and 2940 cm<sup>-1</sup> on the CMC curve are related to the hydrogen bonding-induced hydroxyl (-OH) stretching vibration peak and the methylene (C-H) stretching vibration peak, respectively. The carboxymethyl substituent's carbonyl groups can be seen scissoring at a wavelength of 1588 cm<sup>-1</sup>. The stretching vibration peak induced by the C-H

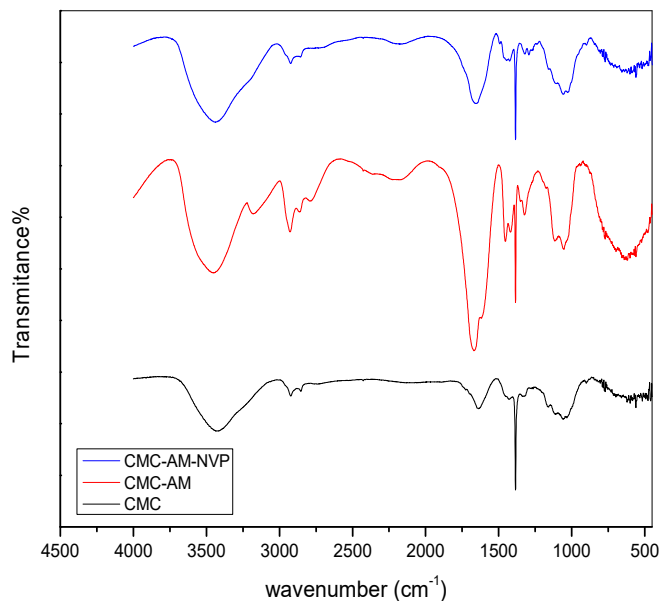


**Fig. 1.** FTIR spectra of used copolymers.

variable angle and the beta-(1,4) glycosidic bond was attributed to the peaks at 1385 cm<sup>-1</sup> and 1066 cm<sup>-1</sup>, respectively. These peaks stand within the typical CMC absorption peaks [17,18]. The presence of acrylamide in the CMC-AM copolymer was validated by the existence of new absorption bands. The curve of these copolymers showed additional absorption bands at 1658 (C=O) and 1609 cm<sup>-1</sup> (NH<sub>2</sub> bending), which can be assigned to the amide groups [14,17]. For the CMC-AM-NVP copolymer curve, we notice that the absorption bands related to the intensity and area of the peak at 3435 cm<sup>-1</sup>, 1658 cm<sup>-1</sup> and 1385 cm<sup>-1</sup> became larger and more pronounced, indicating the presence of the NVP group in the copolymer. Also, the peaks at 1650, 1432, 1260, and 1167 cm<sup>-1</sup> assigned to the C=O stretching of cyclic amide or C=C of NVP, C-H stretching or (-CH<sub>2</sub>-) C-H twist, C-N stretching, and -CH<sub>2</sub>- rocking, respectively [19].

**Thermogravimetric Analysis (TGA).** The thermal stability of the copolymer was examined by TGA, as shown in Fig. 2.

As shown in Fig. 2. It is evident from the TGA curves of the used copolymers that it has three distinct regions of thermal degradation. Water in the sample might cause the polymers to first weigh less than expected. From about 260 °C, there is a second decrease in loss of mass. This was

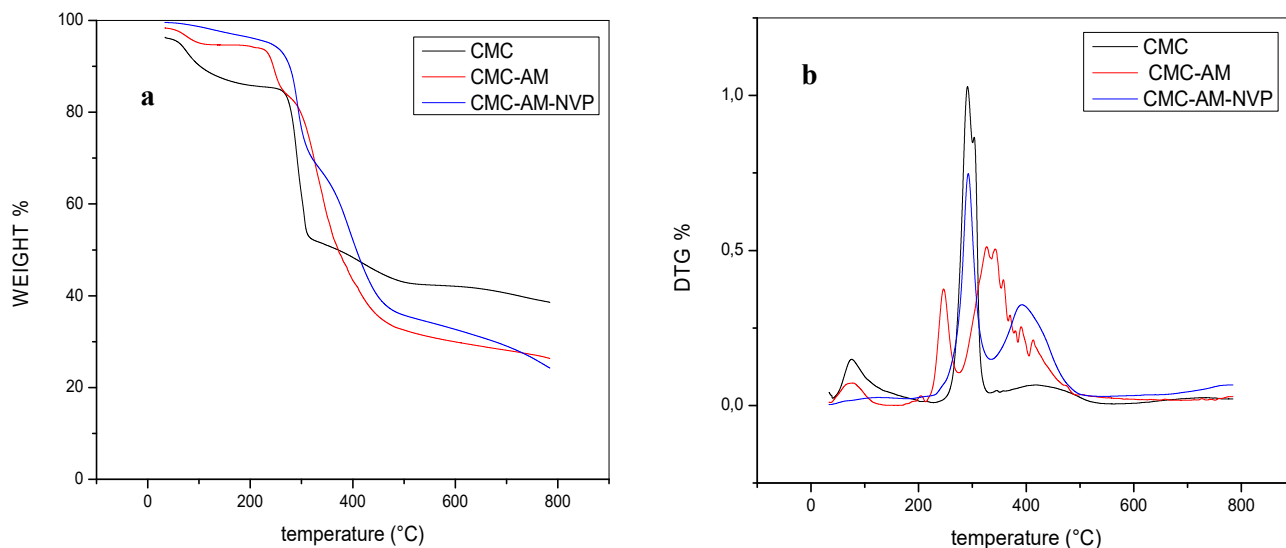


**Fig. 2.** Thermograms of used copolymers. (a) TGA and (b) DTG.

**Table 2.** ATG analysis of Used Copolymers

Specimens	First stage, content (%)	Second stage, content (%)	Third stage, content (%)
CMC	50-207, 12.65	207-329, 38.59	329-535, 15.36
CMC-AM	50-200, 3.17	200-450, 35.73	450-800, 30.95
CMC-AM-NVP	50-200, 5.7	200-450, 72.3	450-800, 11.52

due to the loss of carbon dioxide from the polysaccharide and due to the presence of COO<sup>-</sup> groups in the polysaccharide skeleton; it is decarbonized in this range of temperature. By increasing the temperature above 450 °C, the weight loss may be related to the loss of the hydroxyl groups present on the polysaccharide in the form of water [18-20].

The CMC-AM and the CMC-AM-NVP showed almost the same behavior as CMC. Indeed, from the TGA and DTG curves, they are thermally more stable than CMC. The obtained results are shown in Table 2.

### XRD Analysis

The X-ray patterns of CMC, CMC-AM and CMC-AM-NVP are depicted in Fig. 3. XRD analysis showed that carboxymethyl cellulose exhibits very weak crystallinity around the angle  $2\theta = 21^\circ$  [18,21]. However, the presence of

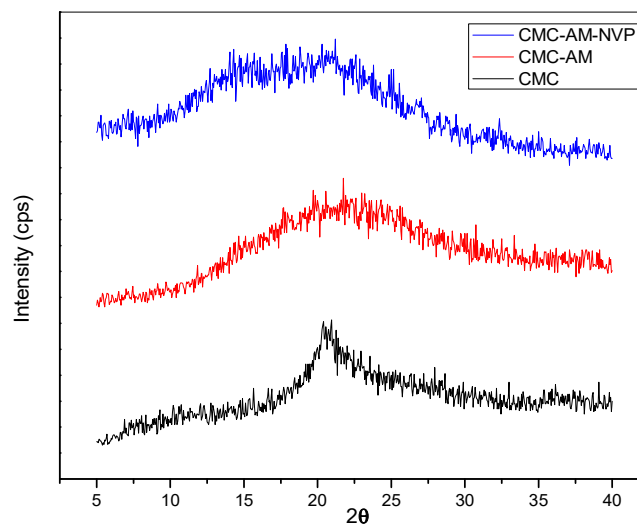


**Fig. 3.** XRD curves of used copolymers.

the broad peak at angle  $2\theta = 15^\circ$  up to  $30^\circ$  confirms the amorphous character of these polymers.

**Surface morphology (SEM).** SEM images of the used copolymers are shown in the Fig. 4.

Similarities between the CMC and the synthesized copolymers were discovered by SEM examination. The CMC was morphologically composed of a smooth-surfaced, individually ordered rod-like structure.

The SEM results for the CMC-AM and the CMC-AM-NVP indicated the shrinking of the hydrogel surface's pore size due to an increase in the monomer content and a decrease in the CMC content. According to the study, the copolymer was found smooth, coherent, and non-porous surface.

## Adsorption Studies

**Effect of pH.** In adsorption studies, an important parameter is the pH of the aqueous solution [22,23]. The initial pH effects on the amount of removed Methylene Blue dye (MB) using three copolymers (CMC, CMC-AM, and CMC-AM-NVP) as adsorbent were studied in the pH range between 2 and 10 at  $25^\circ\text{C}$ . The obtained results are shown in Fig. 5.

The amount of MB dye adsorbed,  $q_e$  ( $\text{mg g}^{-1}$ ), in CMC and CMC-AM reached the maximum of 38.34 and  $38.59 \text{ mg g}^{-1}$ , respectively, at the pH levels above 10. In an acidic medium, the amide group ( $\text{NH}_2$ ) is in the ammonium form  $\text{NH}_3^+$ , which increases the electrostatic repulsion

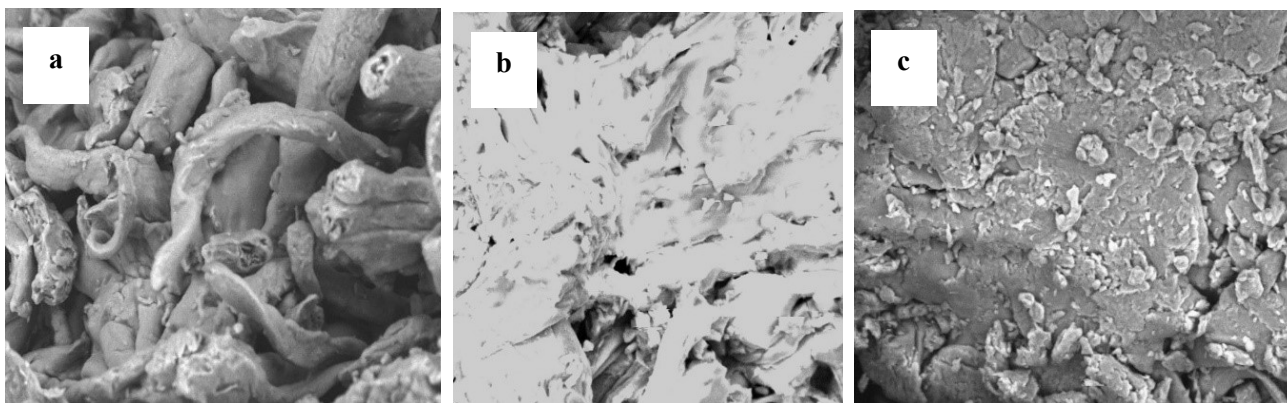


**Fig. 4.** Scanning electron microscope (SEM) image of: a) CMC, b) CMC-AM, c) CMC-AM-NVP.

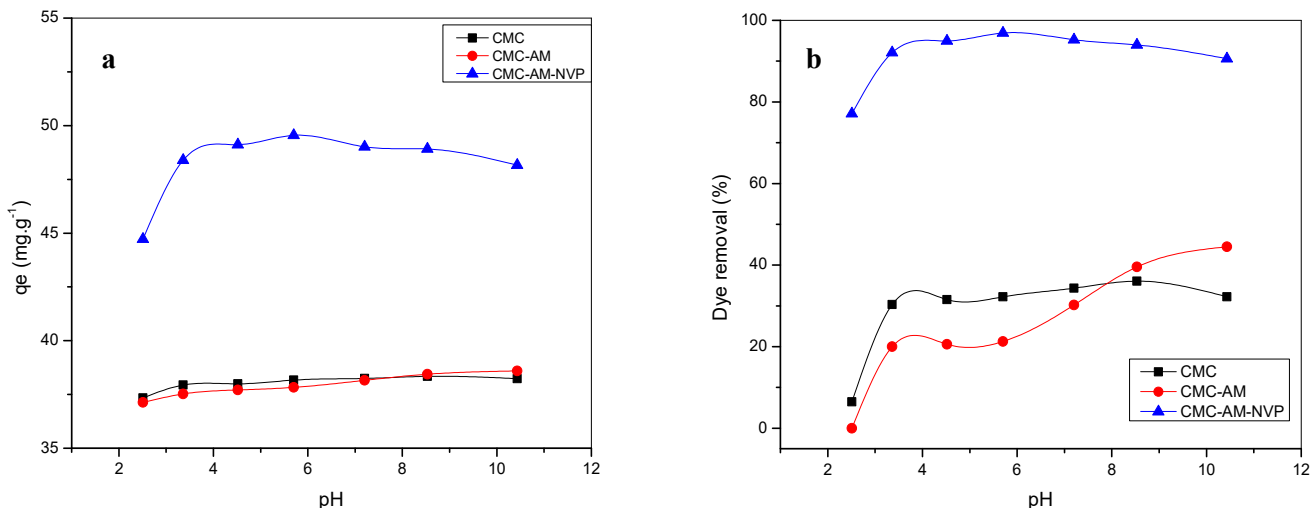
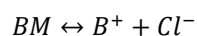


**Fig. 5.** Effect of pH on the adsorption of MB onto the used copolymers. (initial MB concentration =  $20 \text{ mg l}^{-1}$ ,  $m = 0.02 \text{ g}$ ,  $V = 40 \text{ ml}$ , contact time = 120 min,  $T = 293 \text{ K}$ ).

between the positively charged MB dye and the positively charged adsorption sites of the CMC-AM. However, in a basic medium, the  $\text{NH}_2$  group reverts back to its original uncharged state. This leads to an increase in the electrostatic attraction between the positively charged MB dye and the available  $\text{NH}_2$  groups, resulting in the enhanced adsorption on the CMC-AM compared to the CMC alone. In addition, the adsorbed dye amount  $q_e$  ( $\text{mg g}^{-1}$ ) for the CMC-AM-NVP copolymer increased and reached its maximum value at a pH of about 6. This can be explained by the CMC-AM-NVP copolymer's pH of zero-point charge ( $\text{pH}_{\text{PZC}}$ ), which is around 6.44 (results are not shown). At the pH ranges lower and higher than  $\text{pH}_{\text{PZC}}$ , the copolymer has a positive and negative charge, respectively.

In acid pH, the BM molecules are dissociated in solution and organic cations (positively charged) are appeared [24]. Their dissociation can be represented by the following equilibrium:



There is a repulsion between the  $\text{B}^+$  ions of the BM and the positively charged adsorbent sites when these two charges are present. As a result, there are repulsive interactions between the positively charged adsorbent surface and the aromatic cations of BM. Consequently, both the adsorption percentage and  $q_e$  values fall. We observed that an increase in the pH resulted in an increase in the removal capacity and the percentage of the adsorbent. This was obviously caused by a drop in the charge repulsion [24]. Moreover, in basic media, at pH values higher than PZC, the surface charge of CMC-AM-NVP exhibited a tendency to be negative. In addition, the percentage of BM adsorption increased because the electrostatic attraction between the negative adsorbent surface and the organic cations of BM increased. Other interactions that may be present in the adsorption mechanism are the hydrogen bonding interactions of the imine groups of MB molecules ( $\text{RCH}=\text{NR}$ ) with the reactive OH and NH groups of the copolymer [25]. It is worth noting that the BM dye adsorption on these copolymers was consequently better in basic medium than in acid medium. The  $\text{pH} = 5.7$  was considered as the optimum pH for the adsorption of methylene blue on these adsorbents.

### Effect of Contact Time

The  $q_e$  ( $\text{mg g}^{-1}$ ) of the different adsorbents with the BM molecule was also examined by measuring the time at which equilibrium adsorption took place with a fixed amount (20 mg) of adsorbent. As can be seen from Fig. 6, the adsorption of the dye on the adsorbent was increased for more time contact.

We notice from the Fig. 6 that the dye's initial adsorption rate was quick. Due to the free adsorption sites that are available on the adsorbent surface, as soon as the first contact occurs, the adsorption capacity or percentage is increased with contact time. These sites progressively become saturated. In the case of CMC-AM-NVP, the adsorption efficiency attained a value of 80% in less than 50 min, and then it became constant after 60 min. Therefore, it is concluded that the time of 60 min is enough to achieve the equilibrium for the whole study.

### Adsorption Kinetic Models

The kinetic study is crucial to the adsorption process since it enables us to learn more about the mass transfer and adsorption mechanisms. In our research, we used the pseudo-first order, pseudo-second order, and intraparticle diffusion

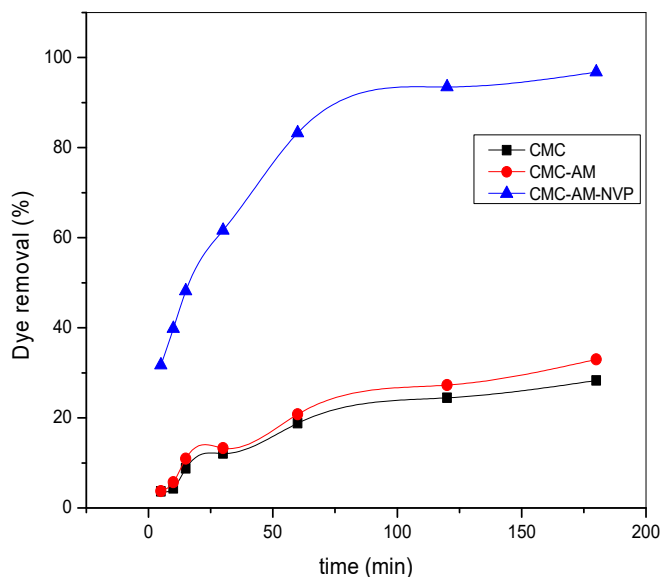


**Fig. 6.** Effect of time on the adsorption of MB dye onto the used copolymers (initial MB concentration =  $20 \text{ mg l}^{-1}$ ,  $m = 0.02 \text{ g}$ ,  $V = 40 \text{ ml}$ ,  $\text{pH} = 5.7$ ,  $T = 293 \text{ K}$ )

kinetic models, which are, respectively, described by the following equations [26,27].

$$\ln(q_e - q_t) = \ln q_e - k_1 t \quad (2)$$

$$\frac{t}{q_t} = \frac{1}{k_2 q_e^2} + \frac{t}{q_e} \quad (3)$$

$$q_t = K_{id} * t^{0.5} + c \quad (4)$$

In above formulations,  $q_e$  is the adsorption efficiency at equilibrium ( $\text{mg g}^{-1}$ ),  $q_t$  ( $\text{mg g}^{-1}$ ) is the adsorbed dye amount

at time ( $t$ ),  $k_1$  ( $\text{min}^{-1}$ ) is the pseudo-first order rate constant,  $k_2$  ( $\text{g mg}^{-1} \text{min}^{-1}$ ) is the pseudo-second order rate constant, and  $K_{id}$  is the intraparticle diffusion rate constant,  $\text{mg} (\text{g}^{-1} \text{h}^{-0.5})$ .

The obtained curves are depicted in Fig. 7. The kinetic variables and correlation coefficient ( $R^2$ ) for the three modeling scheme are reported in Tables 3 and 4.

It is evident from the results that for the first model, the calculated  $q_e$  values were substantially lower than the equivalent experimental values, and the  $R^2$  values were relatively low. Therefore, this model is needed to be revised to simulate the process of MB adsorption onto the three

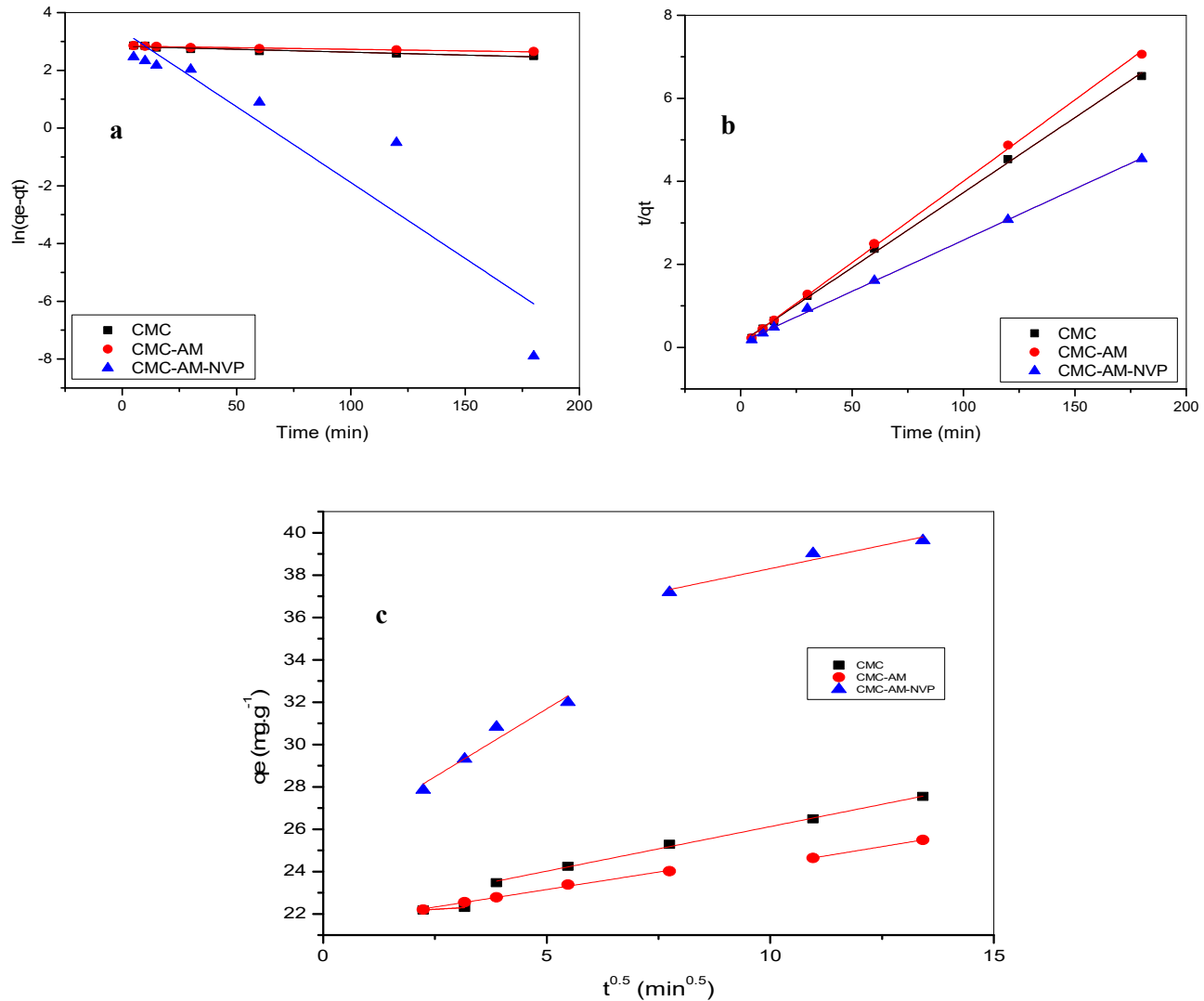


**Fig. 7.** Kinetic model for BM adsorption on used copolymers. a) Pseudo first order, b) pseudo second order and c) the intraparticle diffusion models. (initial MB concentration =  $20 \text{ mg l}^{-1}$ ,  $m = 0.02 \text{ g}$ ,  $V = 40 \text{ ml}$ ,  $\text{pH} = 5.7$ ,  $T = 293 \text{ K}$ ).

**Table 3.** Pseudo-first and Pseudo-second Order Kinetic Parameters for BM Adsorption on Copolymers

Adsorbent	$q_e$ (exp) (mg g <sup>-1</sup> )	Pseudo-first order			Pseudo-second order		
		$k_1$ (min <sup>-1</sup> )	$q_e$ (cal) (mg g <sup>-1</sup> )	$R^2$	$k_2$ (min <sup>-1</sup> )	$q_e$ (cal) (mg g <sup>-1</sup> )	$R^2$
CMC	38.61	0.002	16.77	0.919	0.011	27.68	0.999
CMC-AM	39.44	0.00112	17.11	0.941	0.018	25.51	0.999
CMC-AM-NVP	39.62	0.052	28.80	0.848	0.0052	40.53	0.999

**Table 4.** Intraparticle Diffusion Models Parameters for BM Adsorption on Copolymers

	Intraparticle diffusion					
	$K_{id1}$ (mg g <sup>-1</sup> min <sup>-0.5</sup> )	$C_1$ (mg g <sup>-1</sup> )	$R_1^2$	$K_{id2}$ (mg g <sup>-1</sup> min <sup>-0.5</sup> )	$C_2$ (mg g <sup>-1</sup> )	$R_2^2$
CMC	0.11	21.91	-	0.42	21.91	0,996
CMC-AM	0,33	21.49	0.997	0.34	0.85	-
CMC-AM-NVP	1.28	25.27	0.920	0.43	33.92	0.914

adsorbents. However, it was reported (in the same table) that the  $R^2$  value in the second approach was the highest (above 1), showing that the BM's adsorption on each of the three adsorbents matches well with the pseudo-second order kinetic model. In addition, the pseudo-secondary order kinetic model's calculation of equilibrium capacity ( $q_e$ , cal) was significantly closer to the  $q_e$  measured experimentally. These data indicate that the adsorption rate of MB is highly dependent on the amount of available active adsorption sites [28,29]. In this case, the adsorption rate was mostly controlled by chemical adsorption, which is considered to be a rapid process and a likely reason for the high dye adsorption at lowest concentrations [30].

Furthermore, when the adsorption process includes intraparticle diffusion, three characteristics can be observed: (1) the relationship between the amount of adsorbate adsorbed ( $qt$ ) and the square root of time ( $t^{0.5}$ ) should form a linear plot, (2) in cases where intraparticle diffusion is the dominant step, these linear plots should intersect at the origin, indicating a starting point of adsorption, and (3) if the adsorption process involves multiple steps, there may be two or more distinct slopes observed in the plot [27]. From Fig. 6 c, the adsorption of BM on CMC-AM-NVP occurred in two

steps and showed multilinearity. Rapid adsorption occurred in the first 60 min and then slowed down over the next 120 min.

### Effect of Adsorbent Dosage

Adsorbent mass is an important factor in the study of adsorption, which can help to determine the most cost-effective adsorbent quantity used to remove dangerous contaminants from wastewater [31]. Figure 8 shows the adsorption of MB dye by varying the amounts of adsorbent (10-50 mg) for a 40 ml of dye solution with a concentration of 20 mg l<sup>-1</sup>.

Figure 8 shows an increase in the adsorption rate as a function of the mass of the adsorbent; this quick rise may be attributable to an increase in the number of free adsorption sites with increasing amounts of CMC-AM-NVP up to a mass of 15 mg. The cations of the BM dye may readily access the adsorption sites at low dosages of adsorbent, which accounts for the rapid increase in the adsorbed amount with adsorbent mass. Over this mass value, the number of accessible free sites becomes stable. The addition of adsorbent increases the number of free sites, but it leads to the aggregations of adsorbent particles and excludes some of

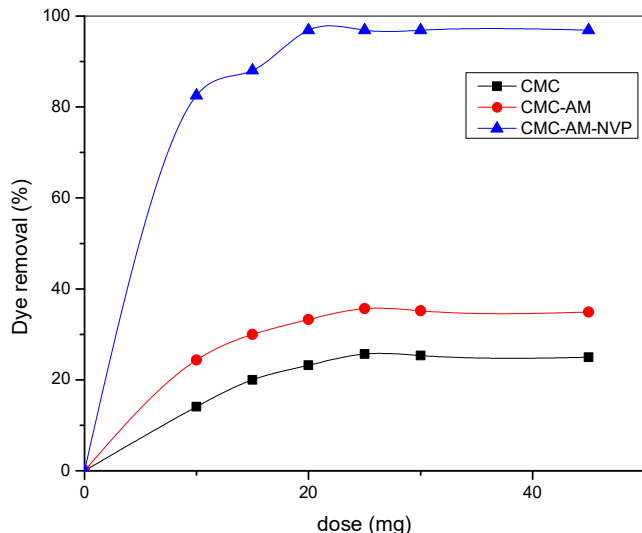


**Fig. 8.** The effect of adsorbent dose on the adsorption of BM dye onto copolymers. (initial MB concentration=20 mg l<sup>-1</sup>, contact time = 60 min, V = 40 ml, pH = 5.7, T = 293 K)

these particles from the adsorption process. The percentage of adsorption was constant up to 50 mg of the added adsorbent [31]. Therefore, a mass of 20 mg was chosen as the optimal dose of adsorbents for the upcoming experiments.

### Initial Dye Concentration Effect

The impact of initial concentration [5 mg l<sup>-1</sup> - 400 mg l<sup>-1</sup>] was studied in a batch mode for BM solution in order to determine the adsorption isotherms. The stirring time is set to 180 min. The obtained results are shown in Fig. 9.

The fact that the dye's adsorption capacity raised as the initial dye concentration raised suggests that the initial dye concentration has an impact on the adsorption process. Therefore, it is concluded that a higher dye concentration can give the dye molecules a stronger push to approach the adsorption sites faster [32].

### Adsorption Isotherm Studies

Adsorption isotherm studies were performed to describe how the adsorbent molecules can interact with dyes. They are important for the optimization of the use of adsorbents [33].

As shown in Fig. 10, at equilibrium concentrations below 2 mg l<sup>-1</sup>, q<sub>e</sub> increased to 100 mg g<sup>-1</sup> for CMC-AM-NVP. Then, it was noticed that the q<sub>e</sub> values increased slowly when

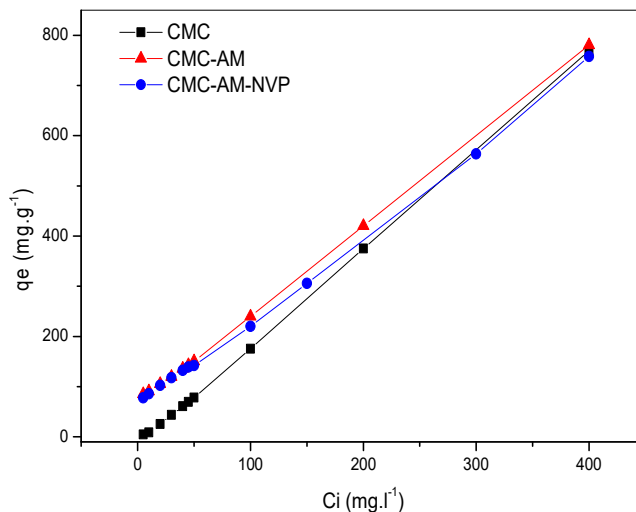


**Fig. 9.** The effect of initial BM concentration on the adsorption capacity onto the copolymers. (m = 0.02 g, contact time = 60 min, V = 40 ml, pH = 5.7, T = 293 K).

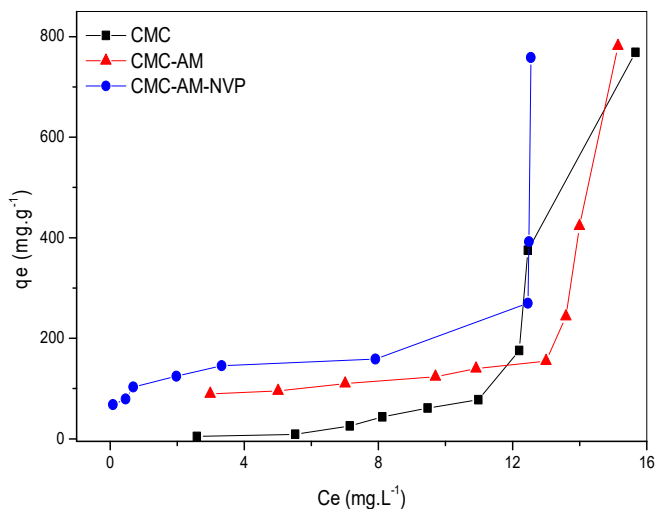


**Fig. 10.** The influence of initial dye concentration on dye adsorption onto used copolymers. (m = 0.02 g, contact time = 60 min, V = 40 ml, pH = 5.7, T = 293 K).

C<sub>e</sub> was in the range of 2 - 12 mg l<sup>-1</sup>. However, when C<sub>e</sub> reached 12 mg l<sup>-1</sup>, q<sub>e</sub> values increased rapidly. These results reveal that C<sub>i</sub> (initial dye concentration) is an influential factor in the adsorption process.

In order to understand the most adequate equilibrium

curve that can be used in the designing of the adsorption mechanism, many models of adsorption isotherms have been formulated by different scientists to predict the applicability of the experimental data. In our case, we used the models of Langmuir, Freundlich and Temkin, which are represented respectively by the following equations [34].

$$\frac{1}{q_e} = \frac{1}{q_{max}} + \frac{1}{C_e \cdot q_{max} \cdot K_L} \quad (5)$$

$$\ln q_e = \ln K_F + \frac{1}{n} \ln C_e \quad (6)$$

$$q_e = \beta \ln K_T + \beta \ln C_e \quad (7)$$

Where

In above formulations,  $C_e$  is the equilibrium concentration of dye ( $\text{mg l}^{-1}$ ),  $q_e$  is the amount of dye adsorbed on the adsorbent ( $\text{mg g}^{-1}$ ),  $K_L$  is the constant of Langmuir model ( $\text{l mg}^{-1}$ ),  $q_{max}$  is the maximum capacity of the adsorbent ( $\text{mg g}^{-1}$ ),  $K_F$  and  $n$  are the constant of Freundlich model, and  $K_T$  and  $\beta$  are Temkin adsorption constant.

The Freundlich isotherm considers that the adsorption process occurs on a heterogeneous surface of the adsorbents, in contrast to the Langmuir model which assumes that it occurs on a homogenous monolayer surface [35]. The adsorbents' surfaces are supposed to be heterogeneous in Temkin's isothermal model, and the heat of adsorption is reduced linearly [26]. The three models' fitted data are depicted in Figs. 11a, 11b, and 11c, respectively. Table 5

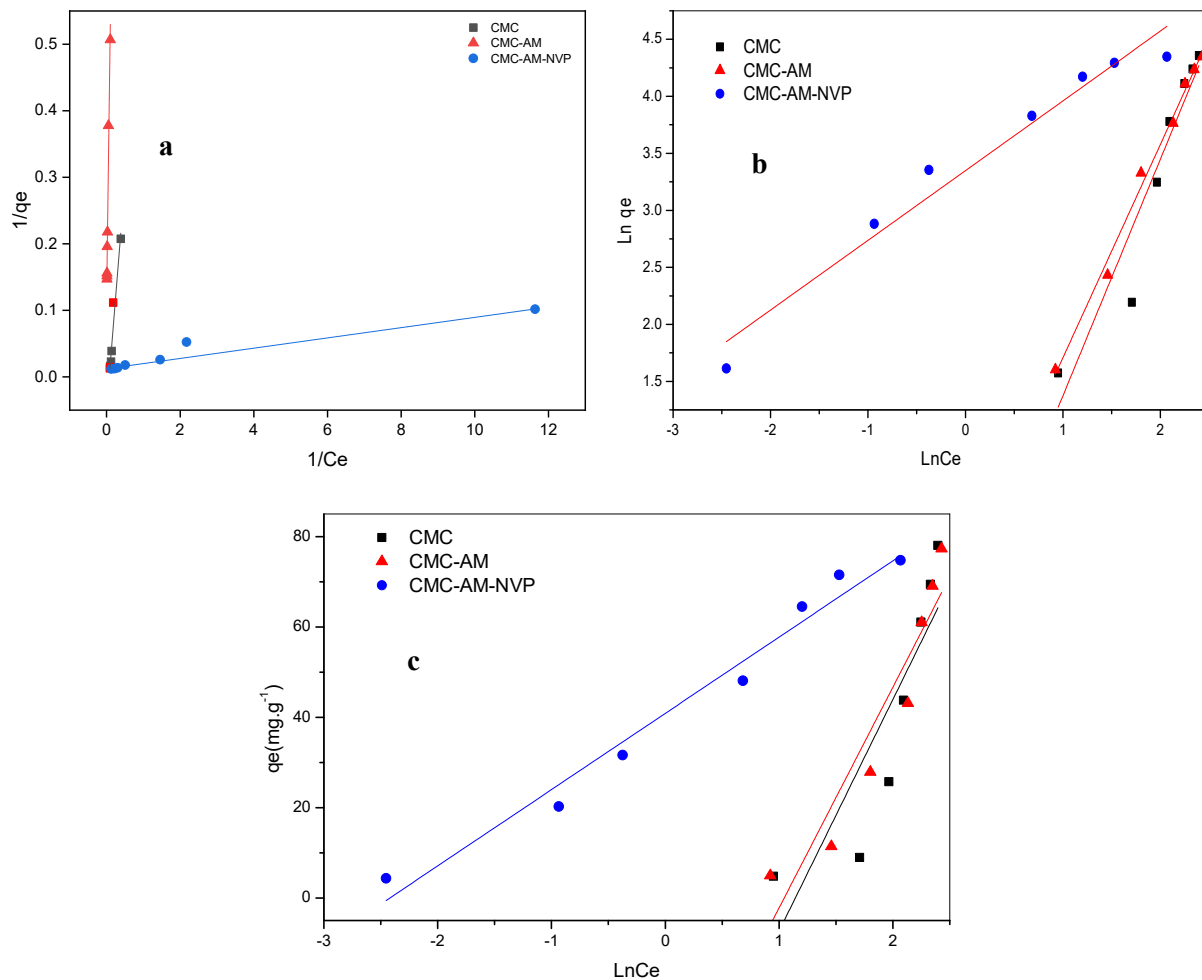


**Fig. 11.** Isotherm plots for the adsorption of BM dye Langmuir plot. b) Freundlich plot. c) Temkin plot ( $m = 0.02 \text{ g}$ , contact time = 60 min,  $V = 40 \text{ ml}$ ,  $\text{pH} = 5.7$ ,  $T = 293 \text{ K}$ ).

**Table 5.** Parameters of the Studied Isotherm for the Adsorption of BM onto Adsorbent

Adsorbent	Langmuir			Freundlich			Temkin		
	$q_m$ ( $\text{mg g}^{-1}$ )	$K_L$ ( $\text{l mg}^{-1}$ )	$R^2$	$K_F$ ( $\text{l g}^{-1}$ )	$1/n$	$R^2$	$K_T$	$\beta$ ( $\text{mg g}^{-1}$ )	$R^2$
CMC	-	-	0,97	0.495	2.07	0,90	0.318	51.26	0,72
CMC-AM	8.92	0.027	0.98	0.848	1.87	0.99	0.351	48.85	0.87
CMC-AM-NVP	81.96	1.58	0.99	38.42	0.48	0.95	15.125	17.81	0.97

summarizes the fitting's derived parameters.

According to these results, it is clear that for the CMC, the R value of the Langmuir models ( $R^2 = 0.97$ ) was significantly higher than that for the Freundlich ( $R^2 = 0.93$ ) and Temkin ( $R^2 = 0.64$ ) models. As a result, it can be concluded that the Langmuir model offers the ideal fit to the results from experiments. Consequently, on the CMC adsorbent surface, a monolayer adsorption occurs.

For the CMC-AM adsorbent, the Langmuir correlation coefficient ( $R^2 = 0.98$ ) was higher than that for the Freundlich ( $R^2 = 0.92$ ) and Temkin ( $R^2 = 0.58$ ) models. This result suggests that Langmuir model is in better agreement with the experimental results and a monolayer adsorption onto the surface of the CMC-AM adsorbent.

The maximum theoretical adsorption capacity ( $q_e$ , cal =  $13.25 \text{ mg g}^{-1}$ ) was closer to the experimental data ( $q_e$ , exp =  $24.35 \text{ mg g}^{-1}$ ). Moreover, the value ( $0 < R_L < 1$ ) showed that the adsorption of the dye molecules on the CMC-AM adsorbent was beneficial. For the CMC-AM-NVP adsorbent, the Langmuir correlation coefficient ( $R^2 = 0.99$ ) was higher than that for the Freundlich ( $R^2 = 0.95$ ) and Temkin ( $R^2 = 0.97$ ) models, suggesting the occurrence of monolayer adsorption by the CMC-AM-NVP adsorbent surface.

For adsorption of dye molecules on the CMC-AM-NVP adsorbent, a significant value of  $K_F$  suggested a high affinity for dye ions, and the value of the empirical parameter  $1/n$  is in the interval  $0.1 < 1/n < 1$ , which indicates a favorable adsorption.  $1/n$  is the slope which indicates the adsorption intensity or surface heterogeneity; a value near zero for  $1/n$  implies a high heterogeneity, a value less than 1 indicates a normal Langmuir isotherm, and a value greater than 1 indicates a physical process [36,37]. As measured by the Langmuir isotherm, the highest adsorption capacities of the CMC, CMC-AM, and CMC-AM-NVP for the dye molecules

were 20.64, 24.35, and  $97.46 \text{ mg g}^{-1}$ , respectively. The CMC-AM-NVP adsorbent was more interesting as adsorbent than pure CMC from a financial point of view.

### Thermodynamic Studies

Thermodynamic tests were conducted at the optimal condition of different temperature to examine how this factor affects the removal of BM by the adsorbents and to learn more about the adsorption process. Thermodynamic parameters were estimated using the following formulae [38]:

$$K_d = q_e/C_e \quad (8)$$

$$\Delta G^\circ = -RT \ln K_d \quad (10)$$

$$\ln K_d = \frac{\Delta S^\circ}{R} - \frac{\Delta H^\circ}{RT} \quad (11)$$

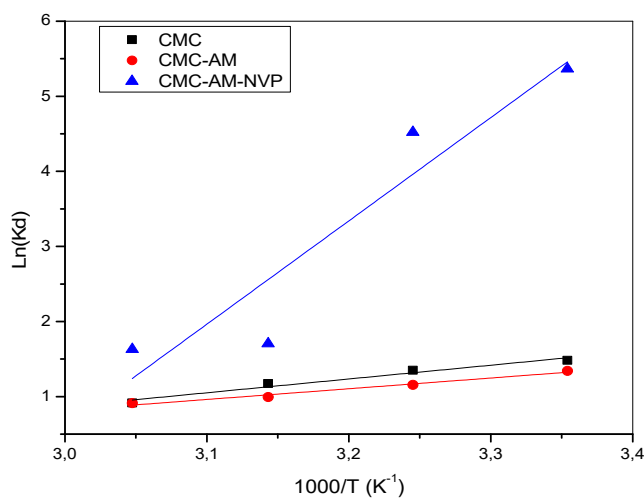
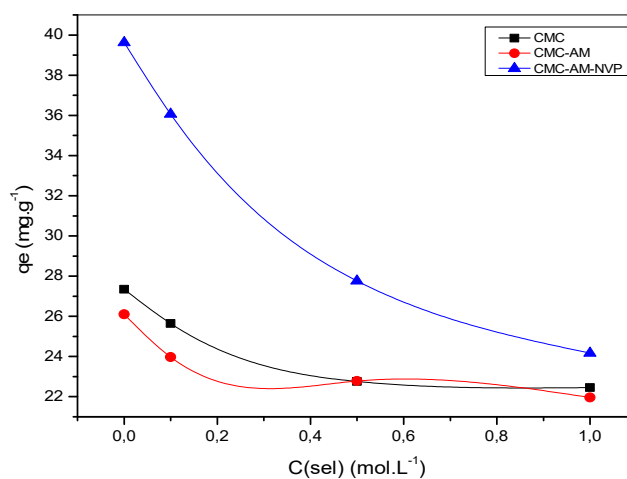
where  $K_d$  is the coefficient of distribution ( $\text{l g}^{-1}$ ); T is the temperature (K), R is the gas constant,  $\Delta H^\circ$  is the enthalpy change ( $\text{kJ mol}^{-1}$ ), and  $\Delta S^\circ$  is the entropy change ( $\text{J mol}^{-1} \text{K}^{-1}$ ).

The plotted  $\ln K_d$  versus  $1/T$  yields reported in Fig. 12 is a linear line from which both enthalpy ( $\Delta H^\circ$ ) and entropy ( $\Delta S^\circ$ ) can be determined from the slope and intercept, respectively. The values of  $\Delta G^\circ$ ,  $\Delta S^\circ$  and  $\Delta H^\circ$  are reported in Table 6.

It can be observed that by elevating the temperature from 25 to 45 °C, the value of  $\Delta G^\circ$  remained negative. These negative values of  $\Delta G^\circ$  suggest that the adsorption process was favorable and naturally spontaneous [39]. The values of  $\Delta H$  were negative, indicating that the adsorption process is exothermic [40]. In addition, the negative  $\Delta S^\circ$  values showed

**Table 6.** Thermodynamic Data for the Adsorption Process of BM at Various Temperatures

Adsorbent	$\Delta H^\circ$ (kJ mol <sup>-1</sup> )	$\Delta S^\circ$ (J mol <sup>-1</sup> K <sup>-1</sup> )	$\Delta G^\circ$ (kJ mol <sup>-1</sup> )			
			298 K	303 K	313 K	323 K
CMC	-15.21	-38.49	-3.674	-3.459	-3.101	-2.455
CMC-AM	-11.80	-28.76	-3.326	-2.990	-2.629	-2.448
CMC-AM-NVP	-114.04	-338.29	-13.30	-11.58	-4.51	-4.44

**Fig. 12.** The Van't Hoff plots for the adsorption. (initial MB concentration = 20 mg l<sup>-1</sup>, m = 0.02 g, contact time = 60 min, V = 40 ml, pH = 5.7).**Fig. 13.** Effect of ionic strength on BM adsorption onto copolymers. (initial MB concentration = 20 mg l<sup>-1</sup>, m = 0.02 g, contact time = 60 min, V = 40 ml, pH = 5.7, T = 293 K).

that there was a diminution of randomness at the solid-solution interface during the adsorption operation [41].

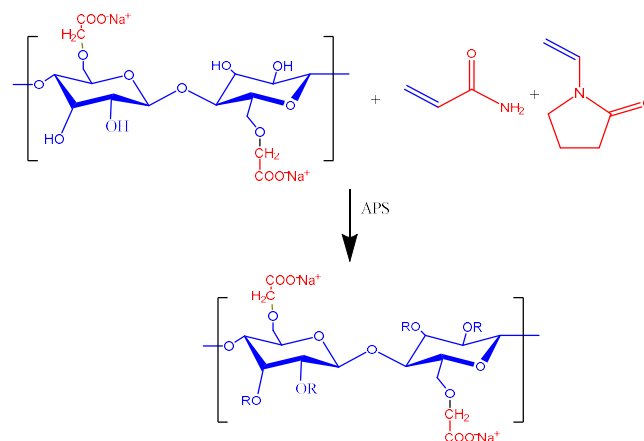
### Effect of Ionic Strength

Dye wastewater usually contains a high amount of salt, so we need to investigate the effect of salt concentration on the percentage of BM removal by our adsorbents.

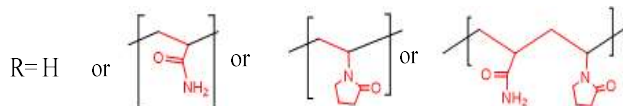
To examine the ionic strength effect on the removal of BM from aqueous solution, the adsorption of BM on all adsorbents was performed by preparing the dye in a salt solution (KCl) at different concentration (0.1 M, 0.5 M and 1 M). The obtained results are shown in Fig. 13. It can be noted that the percentage of removal decreased by an increase in the concentration of salt. This decrease may be caused by an increase in the electrostatic interaction between the adsorbents and salt ions.

### Proposed Adsorption Mechanism

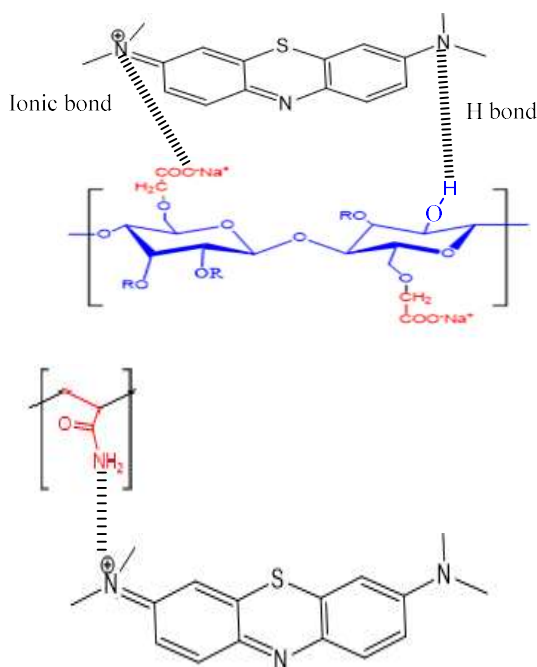
In this study, the copolymer is composed of CMC, AM and NVP. The reaction mechanism and the synthesis route are presented in the following figure.



With



The adsorption can be affected by the hydrogen bonding that can take place between the oxygen groups of the CMC as well as the functional groups of AM and NVP and the nitrogen (N) and oxygen (O) of the dye. Therefore, the excellent adsorption properties of the copolymer may be due to the cooperative impact of both electrostatic and hydrogen bonding between the copolymer and the MB dye.



## CONCLUSION

The CMC-AM-NVP copolymer was synthesized using the free radical polymerization method and was characterized by FTIR, ATG, and DRX. The methylene blue (MB) dye adsorption on this copolymer was studied under various experimental conditions including contact time, pH medium, adsorbent dose, initial dye concentrations, and temperature. The kinetics study followed the pseudo-second order model, and the Langmuir model was in better agreement with the

experimental data. The effect of temperature showed that the MB adsorption process was exothermic. The cost-effectiveness, excellent adsorption, and catalytic properties proved that our copolymer is a promising material for the wastewater treatment.

## REFERENCES

- [1] Gök, M. K.; Güçlü, G., Removal of Basic Dye from Aqueous Solutions Using a Novel Nanocomposite Hydrogel: N-Vinyl-2-Pyrrolidone/Itaconic Acid/Organo Clay. *Water, Air, & Soil Pollution*, **2013**, *224*, 11, DOI: 10.1007/s11270-013-1760-5.
- [2] Radhy, N. D.; Jasim, L. S., Synthesis of Graphene Oxide/Hydrogel Composites and Their Ability for Efficient Adsorption of Crystal Violet. *J. Pharm. Sci. & Res.* **2019**, *11*, 456-463, DOI: jpsr11021936.pdf.
- [3] Khadhraoui, M.; Trabelsi, H.; Ksibi, M.; Bouguerra, S.; Elleuch, B., Discoloration and detoxification of a Congo red dye solution by means of ozone treatment for a possible water reuse. *J. Hazard. Mater.* **2009**, *161*, 974-981, DOI: 10.1016/j.jhazmat.2008.04.060.
- [4] Cruz-Silva, R.; Endo, M.; Terrones, M., Graphene oxide films, fibers, and membranes. *Nanotechnol. Rev.* **2016**, *5*, 377-391, DOI: 10.1515/ntrev-2015-0041.
- [5] Gopinath, K. P.; Murugesan, S.; Abraham, J.; Muthukumar, K., Bacillus sp. mutant for improved biodegradation of Congo red: Random mutagenesis approach. *Bioresour. Technol.* **2009**, *100*, 6295-6300, DOI: 10.1016/j.biortech.2009.07.043.
- [6] Hocine. T.; Benabadji, K. I.; Bouras, B., Zennaki, A.; Benali, A., Enhanced Removal of Brilliant Orange by Poly(4-vinylpyridine)/Acid-Activated Bentonite Composite. *Phys. Chem. Res.* **2023**, *11*, 327-339, DOI: 10.22036/pcr.2022.340830.2096
- [7] Aljeboree, A. M.; Alshirifi, A. N.; Alkaim, A. F., Kinetics and equilibrium study for the adsorption of textile dyes on coconut shell activated carbon. *Arab. J. Chem.*, **2017**, *10*, 3381-3393, DOI: 10.1016/j.arabjc.2014.01.020.
- [8] Baouch, Z.; Benabadji, K. I.; Bouras, B., Adsorption of different dyes from aqueous solutions using organoclay. *Phys. Chem. Res.* **2020**, *8*, 767-787, DOI: 10.22036/pcr.2020.234691.1787.

- [9] Medjahed, K.; Tennouga, L.; Mansri, A.; Chetouani, A.; Hammouti, B.; Desbrières, J., Interaction between poly(4-vinylpyridine-graft-bromodecane) and textile blue basic dye by spectrophotometric study. *Res. Chem. Intermed.* **2013**, *39*, 3199-3208, DOI: 10.1007/s11164-012-0832-2.
- [10] Zhu, H. Y.; Jiang, R.; Fu, Y. Q.; Jiang, J. H.; Xiao, L.; Zeng, G. M., Preparation, characterization and dye adsorption properties of  $\gamma$ -Fe<sub>2</sub>O<sub>3</sub>/SiO<sub>2</sub>/chitosan composite. *Appl. Surf. Sci.* **2011**, *258*, 1337-1344, DOI: 10.1016/j.apsusc.2011.09.045.
- [11] Varaprasad, K.; Jayaramudu, T.; Rotimi, E., Removal of dye by carboxymethyl cellulose, acrylamide and graphene oxide via a free radical polymerization process Removal of dye by carboxymethyl cellulose, acrylamide and graphene oxide via a free radical polymerization process. *Carbohydr. Polym.* **2017**, *164*, 186-194, 2017, DOI: 10.1016/j.carbpol.2017.01.094.
- [12] Lan, W.; He, L.; Liu, Y., Preparation and Properties of Sodium Carboxymethyl Cellulose/Sodium Alginate/Chitosan Composite Film. *Coatings.* **2018**, *8*, 291, DOI: 10.3390/coatings8080291.
- [13] Feng, X; Wan, J.; Deng, J.; Wenshu Q., Preparation of acrylamide and carboxymethyl cellulose graft copolymers and the effect of molecular weight on the flocculation properties in simulated dyeing wastewater under different pH conditions. *Int. J. Biol. Macromol.* **2020**, *15*, 1142-1156, DOI: 10.1016/j.ijbiomac.2019.11.081
- [14] Godiya, C. B.; Cheng, X.; Li, D.; Chen, Z.; Lu, X., Carboxymethyl cellulose/polyacrylamide composite hydrogel for cascaded treatment/reuse of heavy metal ions in wastewater Carboxymethyl cellulose/polyacrylamide composite hydrogel for cascaded treatment/reuse of heavy metal ions in wastewater. *J. Hazard. Mater.* **2018**, *364*, 28-38, DOI: 10.1016/j.jhazmat.2018.09.076.
- [15] Zou, Y.; Shanshan, L.; Yuqi, W.; Chenxi, Y., Flocculation behavior of cationic pea starch prepared by the graft copolymerization of acrylamide for wastewater treatment. *J. Appl. Polym. Sci.* **2016**, *133*, 43922, 1-11, DOI: 10.1002/app.43922.
- [16] Mehiaoui, L.; Benali, A.; Tennouga, L.; Bouras, B.; Medjahed, K., Polyelectrolyte Complexes Formation Based On Carboxymethylcellulose Sodium Salt (NaCMC) And Quaternized Poly (4-Vinylpyridine) (Qp4VP). *Rev. Roum. Chim.* **2021**, *66*, 399-407, DOI: 10.33224/rrch.2021.66.5.02.
- [17] Belaid, A.; Bouras, B.; Hocine, T.; Tennouga, L., Flocculation of Clay Suspensions Using Copolymers Based on Acrylamide and Biopolymer. *Phys. Chem. Res.* **2023**, *11*, 221-230, DOI: 10.22036/PCR.2022.331188.2036
- [18] Varaprasad, K.; Jayaramudu, T.; Sadiku, E. R., Removal of dye by carboxymethyl cellulose, acrylamide and graphene oxide via a free radical polymerization process. *Carbohydr. Polym.*, **2017**, *164*, 186-194, DOI: 10.1016/j.carbpol.2017.01.094.
- [19] Luo, Y. L.; Xu, F.; Chen, Y. S.; Jia, C. Y., Assembly, characterization of Ag nanoparticles in P(AAm-co-NVP)/CS semi-IPN, and swelling of the resulting composite hydrogels. *Polym. Bull.* **2010**, *65*, 181-199, DOI: 10.1007/s00289-010-0248-3.
- [20] Tripathy, T., Synthesis of Polyacrylamide Grafted Carboxymethylcellulose and Evaluation of Its Flocculation Characteristics. *Int. J. Polym. Mat. Polym. Biomat.* **2007**, *56*, 461-482, DOI: 10.1080/00914030600904660.
- [21] Yue, Y.; Zheng, L.; Wang, Y.; Wu, J.; Li, S.; Han, X.; Wu, L., A novel polyamidine-grafted carboxymethylcellulose: synthesis, characterisation and flocculation performance test. *e-Polymers.* **2019**, *19*, 225-234, DOI: 10.1515/epoly-2019-0023.
- [22] Youssef, B.; Soumia, A.; Mounir, E.; Omar, C.; Abdelaziz, L.; Mehdi, E.; Mohamed, Z., Preparation and properties of bionanocomposite films reinforced with nanocellulose isolated from moroccan alfa fibres. *Aut. Res. J.* **2015**, *15*, 164-172, DOI: 10.1515/aut-2015-0011.
- [23] Patel, Y. N.; Patel, M. P., Novel cationic poly[AAM/NVP/DAPB] hydrogels for removal of some textile anionic dyes from aqueous solution. *J. Macromol. Sci. Part A Pure Appl. Chem.* **2012**, *49*, 490-501, DOI: 10.1080/10601325.2012.676915.
- [24] Binaeian, E., Tayebi, H. A.; Shokuhi Rad, A.; Afrashteh, S., Adsorption of acid blue on synthesized polymeric nanocomposites, PPy/MCM-41 and PAni/MCM-41: Isotherm, thermodynamic and kinetic

- studies. *J. Macromol. Sci. Part A Pure Appl. Chem.* **2018**, *55*, 269-279, DOI: 10.1080/10601325.2018.1424554.
- [25] Kifuani, K. M.; Mayeko, A. K. K.; Vesituluta, P. N.; Lopaka, B. I.; Bakambo, G. E.; Mavinga, B. M.; Lunguya, J. M., Adsorption d' un colorant basique , Bleu de Méthylène, en solution aqueuse , sur un bioadsorbant issu de déchets agricoles de Cucumeropsis mannii Naudin. *Int. J. Bio. Chem. Sci.* **2018**, *12*, 558-575, DOI: 10.4314/ijbcs.v12i1.43.
- [26] Thakur, S.; Pandey, S.; Arotiba, O. A., Development of a sodium alginate-based organic/inorganic superabsorbent composite hydrogel for adsorption of methylene blue. *Carbohydr. Polym.* **2016**, *153*, 34-46, DOI: 10.1016/j.carbpol.2016.06.104.
- [27] Salari, H.; Erami, M.; Dokoohaki, M. H. ; Zolghadr, A. R., New insights into adsorption equilibrium of organic pollutant on MnO<sub>2</sub> nanorods: Experimental and computational studies. *J. Molecular. Liquids.* **2022**, *345*, 117016, DOI: 10.1016/j.molliq.2021.117016
- [28] Wei, H.; Sun, J.; Zhang, B.; Liu, R., Comparative Study of Cationic Dye Adsorption Using Industrial Latex Sludge with Sulfonate and Pyrolysis Treatment. *Sustainability.* **2020**, *12*, 10048, DOI: 10.3390/su122310048.
- [29] Oussalah, A.; Boukerroui, A.; Aichour, A.; Djellouli, B., Cationic and anionic dyes removal by low-cost hybrid alginate/natural bentonite composite beads: Adsorption and reusability studies. *Int. J. Biol. Macromol.* **2019**, *124*, 854-862, DOI: 10.1016/j.ijbiomac.2018.11.197.
- [30] Fabryanty, R.; Valencia, C.; Edi, F.; Nyoo, J., Removal of crystal violet dye by adsorption using bentonite-alginate composite. *J. Environ. Chem. Eng.* **2017**, *5*, 5677-5687, DOI: 10.1016/j.jece.2017.10.057.
- [31] Han, S.; Liu, K.; Hu, L.; Teng, F.; Yu, P.; Zhu, Y., Superior Adsorption and Regenerable Dye Adsorbent Based on Flower-Like Molybdenum Disulfide Nanostructure. *Sci. Rep.* **2017**, *7*, 43599, DOI: 10.1038/srep43599.
- [32] Mittal, H.; Parashar, V.; Mishra, S. B.; Mishra, A. K., Fe<sub>3</sub>O<sub>4</sub> MNPs and gum xanthan based hydrogels nanocomposites for the efficient capture of malachite green from aqueous solution. *Chem. Eng. J.* **2014**, *255*, 471-482, DOI: 10.1016/j.cej.2014.04.098.
- [33] Aminu, I.; Gumel, S. M.; Ahmad, W. A.; Idris, A. A., Adsorption Isotherms and Kinetic Studies of Congo-Red Removal from Waste Water Using Activated Carbon Prepared from Jujube Seed. *Amer. J. Analyt. Chem.* **2020**, *11*, 47-59, DOI: 10.4236/ajac.2020.111004.
- [34] Olasehinde, E. F.; Abegunde, S. M.; Adebayo, M. A., Adsorption isotherms, kinetics and thermodynamic studies of methylene blue dye removal using Raphia taedigera seed activated carbon. *Casp. J. Environ. Sci.* **2020**, *18*, 329-344, DOI: 10.22124/cjes.2020.4279.
- [35] Obaid, S. A., Langmuir, Freundlich and Tamkin Adsorption Isotherms and Kinetics For The Removal Aartichoke Tournefortii Straw From Agricultural Waste. *J. Phys. Conf. Ser.* **2020**, *1664*, 012011, DOI: 10.1088/1742-6596/1664/1/012011.
- [36] Sizirici, B.; Yildiz, I.; Alyammahi, A.; Obaidalla, F.; Almehairbi, M.; Alkhajeh, S., Adsorptive removal capacity of gravel for metal cations in the absence/presence of competitive adsorption. *Environ. Sci. Pollut. Res.* **2018**, *25*, 7530-7540, DOI: 10.1007/s11356-017-0999-6.
- [37] El-Sayed, G. O., Removal of methylene blue and crystal violet from aqueous solutions by palm kernel fiber. *Desalination.* **2011**, *272*, 225-232, DOI: 10.1016/j.desal.2011.01.025
- [38] Marrakchi, F.; Bouaziz, M.; Hameed, B. H., Adsorption of acid blue 29 and methylene blue on mesoporous K<sub>2</sub>CO<sub>3</sub>-activated olive pomace boiler ash. *Colloids. Surf. A Physicochem. Eng. Asp.* **2017**, *535*, 157-165, DOI: 10.1016/j.colsu rfa.2017.09.014
- [39] Fu, j.; Zhu, J.; Wang, Z.; Wang, Y.; Wang, S.; Yan, R.; Xu, Q., Highly-efficient and selective adsorption of anionic dyes onto hollow polymer microcapsules having a high surface-density of amino groups: isotherms, kinetics, thermodynamics and mechanism. *J. Colloid Interface Sci.* **2019**, *542*, 123-135, DOI: 10.1016/j.jcis.2019.01.131.
- [40] Farman, A.; Nisar, A.; Iram, B.; Amir, S.; Shahid, N.; Zarshad, A.; Syed, M. S.; Hafiz, M. N. I.; Muhammad, B., Adsorption isotherm , kinetics and thermodynamic of acid blue and basic blue dyes onto activated charcoal. *Case Studies Chem. Environ. Eng.* **2020**, *2*, 100040,

DOI: 10.1016/j.cscee.2020.100040.

[41] Benhouria, A.; Islam, A.; Zaghouane-Boudiaf, H.; Boutahala, M.; Hameed, B. H., Calcium alginate-

bentonite-activated carbon composite beads as highly effective adsorbent for methylene blue. *Chem. Eng. J.* **2015**, *270*, 621-630, DOI: 10.1016/j.cej.2015.02.030.